Addition of Graphene on the Bacterial Cellulose Nanocomposite Membrane with Copper Oxide Reinforcement

Maulana, Jibril
Center of Excellence for Cellulose Composite (CECCom), Department of Mechanical and Industrial Engineering, Universitas Negeri Malang

Suryanto, Heru
Center of Excellence for Cellulose Composite (CECCom), Department of Mechanical and Industrial Engineering, Universitas Negeri Malang

Aminnudin
Department of Mechanical and Industrial Engineering, Universitas Negeri Malang

J. S. Binoj
Institute of Mechanical Engineering, Saveetha School of Engineering, Saveetha Institute of Medical and Technical Sciences (SIMATS)

https://doi.org/10.5109/7172255

出版情報：Evergreen. 11 (1), pp.186-194, 2024-03. 九州大学グリーンテクノロジー研究教育センター
バージョン：

Addition of Graphene on the Bacterial Cellulose Nanocomposite Membrane with Copper Oxide Reinforcement

Jibril Maulana[1], Heru Suryanto[1*], Aminnudin[2], J. S. Binoj[3]

[1]Center of Excellence for Cellulose Composite (CECCom), Department of Mechanical and Industrial Engineering, Universitas Negeri Malang, Jl. Semarang No 5 Malang, 65145, Indonesia

[2]Department of Mechanical and Industrial Engineering, Universitas Negeri Malang, Jl. Semarang No 5 Malang, 65145, Indonesia

[3]Institute of Mechanical Engineering, Saveetha School of Engineering, Saveetha Institute of Medical and Technical Sciences (SIMATS), Chennai, India

*Author to whom correspondence should be addressed:
E-mail: heru.suryanto.ft@um.ac.id

(Received September 20, 2023; Revised January 04, 2024; Accepted March 16, 2024).

Abstract: Pineapple peel waste may be utilized as a source of cellulose. This research work presents pineapple peel waste utilization to produce Bacterial Cellulose (BC) as a nanocomposite membrane with Copper Oxide (CuO) and Graphene reinforcement. The procedure involved crushing and homogenizing BC, followed by adding CuO and Graphene. The membrane analysis used XRD, FTIR, SEM, roughness, and tensile test. The results indicated that Graphene reduces the crystallinity and roughness of the membrane. The experiments revealed a strong link between BCNC, CuO, and Graphene, which increases the membrane strength. So, the BCNC/CuO/Graphene can be used as filter candidates.

Keywords: Bacterial Cellulose; Nanocomposite; CuO; Graphene

1. Introduction

Cellulose is a biopolymer obtained from bioresources such as plants and wood, some species of algae, and bacteria [1)]. The global cellulose market reached USD219.53 billion in 2018 and is predicted to increase to USD305.08 billion in 2026 [2)]. One particular type of cellulose readily available in the natural environment is bacterial cellulose (BC). BC fiber has a diameter of 25-86 nm [3)]. The most often used BC uses are in the fields of bioengineering, cosmetics, and biomedicine. BC is a natural polymer that is widely used [4)]. *Acetobacter xylinum* bacteria created it from pineapple peel extract fermentation [5)]. Thermal and chemical stability, biodegradability, hydrophilicity, mechanical strength, and high crystallinity are the most intriguing features of BC [6)]. When compared to other natural celluloses, BC has the most significant cellulose percentage, close to 100% [7)]. Bacterial nanocellulose (BCNC) is obtained from disintegration and homogenization using a high-pressure homogenizer machine and can be nanosizing cellulose until a fiber diameter of approximately 35-55 nm [8)]. Nanocellulose is cellulose that is nanoscale in size. It can be micro-fibrillated cellulose, also known as cellulose nanofibers, nanocrystalline cellulose, or bacterial nanocellulose, which refers to bacteria-produced nano-structured cellulose.

Polymer composites have recently been introduced by combining several types of inorganic filler substances into polymeric frameworks[9)]. CuO, among various materials, stands out with its exceptional characteristic combinations. This material has high erosion resistance, extraordinary temperature harmony, high and flexible modulus, and efficient electrical and thermal conductivity, significantly improving polymeric materials' secondary properties [10,11)].

Copper, a metal known for its antibacterial properties, exhibits a cost advantage over silver. Moreover, copper has the unique ability to directly target bacterial cell membranes and infiltrate bacterial tissues [12)]. CuO's functionality as a reinforcing agent in polymers can be improved through hybridization with Graphene. Graphene and its derivatives exhibit outstanding mechanical characteristics, rendering them a superior choice for the development of materials [13)]. In a distinct research endeavor, Graphene was harnessed to augment the mechanical robustness of a bacterial cellulose (BC) membrane, yielding a substantial enhancement of 2–3 times in comparison to the mechanical strength observed in the BC sample [14)]. Through the incorporation of Graphene into the BCNC/CuO network, there is an anticipation of augmenting the properties of the resulting BCNC/CuO polymer, particularly with regard to its

mechanical strength.

The synthesis methods, characteristics, and applications of nanocellulose hybrids with diverse metal oxide nanoparticles, such as Graphene, are discussed in this article [15]. Graphene, a carbon-based two-dimensional (2D) material, has excellent electrical, mechanical, and thermal properties, as well as a high surface-to-volume ratio [16]. It has a modulus young of 1000 GPa and a fracture strength of 125 GPa. Graphene has numerous applications in electronics and polymer reinforcement. The purpose of this work was to see how introducing Graphene affected the morphology, crystallinity of cellulose, intermolecular bonding, tensile strength, and membrane surface roughness from pineapple peel.

2. Materials and Method

Materials

The pineapple peel used in this research was purchased from the local market in Malang, East Java, Indonesia. *Acetobacter xylinum* as a cellulose starter, sugar, urea, and the surfactant of CTAB was supplied by Merck, Germany. The Copper Oxide nanoparticles were procured from Material Tech. Co., Ltd. in Guangzhou Hongwu, China, with particles size around 30-50 nm, while the Graphene was sourced from SkySpring Nanomaterials, Inc. in the USA with thickness particles around 5nm.

Bacterial Cellulose Synthesis

The synthesis process was based on a methodology employed in earlier studies conducted by Maulana et al. [10]. Initially, pineapple peels 300 grams of pineapple peel are finely crushed using a blender along with 2 liters of water to obtain pineapple peel extract. After obtaining the pineapple peel extract, 5 grams of urea and 150 grams of sugar are introduced and mixed into the mixture, which is then boiled. Boiling is done to facilitate the dissolution of the sugar and urea into the extract. Subsequently, once the mixture has cooled down to a temperature of 30°C, a 20% bacterial starter is incorporated into the medium, and this fermentation process is carried out for 14 days.

Homogenization Process

The pellicle was stirred in 1% NaOH solvent for 120 minutes at 90°C before homogenization to clean from impurities[17]. After cleaning pellicles, every 50 grams of pellicle was crushed with 1 liter of water for 5 minutes during the homogenization process. Then, BC solvents were homogenized using a Nano-Homogenizer machine (AH-100D, Berkley Scientific, China) with a 150 bar pressure and repeated five times[18]. The solution was filtered to obtain bacterial nanocellulose.

Nanocomposite Synthesis

3 grams of filtered bacterial nanocellulose were stirred in 200ml distilled water. After 10 minutes, the 2% CuO and 1% CTAB were added to the BC solution. Variation of Graphene with composition in 0.1%, 0.3%, and 0.5% from BC (w/w) added to 200 ml of BCNC/CuO solvent and then stirred for 1 hour. It was homogenized using an ultrasonic homogenizer for 30 minutes with power 80% from 24kHz. The Bacterial Cellulose Nanocomposite (BCNC) membrane was dried through a freeze-drying over a span of 3 days.

Morphology Analysis

The morphology analyzed by SEM reveals a range of characteristics related to the characteristics of the composite [19]. The morphology observations were conducted using Scanning Electron Microscopy (SEM), specifically the Inspect-S50 type from FEI, with an enlargement of 100,000 times. Prior to the examination, a 10 nm gold coating was applied to the composite membrane's surface. This coating enhanced the membrane surface's conductivity and provided clarity in visualizing the surface morphology of the nanocomposite.

Crystallinity Analysis

The analysis of BCNC involved X-ray Diffraction (XRD) using the PANalytical Expert-Pro instrument. Subsequently, the obtained calculations were subjected to analysis using the Scherer and Segal equations. The XRD test was conducted over a range of 2Theta angles spanning from 5 degrees to 50 degrees. The Segal equation, as depicted in equations 1 and 2, was used to determine crystallinity properties.

$$Cr = \frac{I_{(002)}}{I_{(002)} + I_{(am)}} x100\% \quad (1)$$

$$CI = \frac{I_{(002)} - I_{(am)}}{I_{(002)}} x100\% \quad (2)$$

We define $I_{(am)}$ to represent the amorphous intensity at 18° and $I_{(002)}$ to represent the crystalline at 22°–23°.

FTIR Analysis

The BCNC membranes display periodic variations in their molecular bonds and functional groups, which are detectable through the Fourier Transform Infrared Spectroscopy (FTIR) test. The composite membrane was subjected to FTIR scanning to assess the specific functional groups present in the composite membrane, covering a wavenumber range from 400 to 4000 cm^{-1}. Subsequently, the FTIR data obtained were compared to an IR Correlation Table to identify and characterize the unique functional groups within the membrane[20] .

Mechanical Strength Testing

A fundamental Tensile Strength test refers to applying a specimen to uniaxial stress until the material breaks[21]. The tensile test was conducted following the ASTM D638-V standard[22]. The experiment was conducted on three separate occasions. The result of the tensile test was

averaged. Mechanical testing was executed using a fiber-based tensile test apparatus with a maximum force capacity of 50 N. Samples were prepared by cutting them according to the specifications outlined in ASTM D638-V and securely placed within the grips of the tensile tester for evaluation.

Surface Roughness Testing

For the observation effect of adding CuO and Graphene, the BCNC membrane surface was tested with Surftest SJ-301, Mitutoyo Co, Japan, with a precision gauge of 0.75 mN. The horizontal roughness value rate was 200.0 µm/cm, and the vertical roughness value rate was 5.0 µm/cm.

3. Result and Discussion

Morphology Analysis of BCNC/CuO/Graphene

CuO results in aggregation in the nanocomposite at various locations. This was related to the addition of CuO, which caused CTAB binding to be incompletely dispersed, resulting in CuO aggregation [11,23]. Figure 1 shows the incorporation of Graphene into the bacterial cellulose and CuO nanocomposite network. The dark flat plates, which are depicted as Graphene, can be seen filling the porosity of the BCNC/CuO network. As seen in Figure 1, Graphene also forms numerous bonds with CuO, as evidenced by the attachment of CuO particles to Graphene [24]. This is evidence that CuO can have bonding with Graphene [25].

Analysis Crystallinity of BCNC/CuO/Graphene

The crystallinity of BCNC was affected by the addition of Graphene. The addition of Graphene causes a decrease in the intensity at 22.6° [26], which means that the Graphene can reconstruct the cellulose network and affect the mechanical properties of BCNC, and in this case, is BCNC/CuO [27]. Figure 2 and Table 1 show the effect of adding Graphene to BCNC/CuO in detail.

The addition of Graphene appears to cause straight bumps with no peaks at a diffraction angle of 13.7°, implying single-layer Graphene with a miller index $(1\bar{1}0)$ [26,28]. Because of the amorphous nature of single-layer Graphene and the low quantity in the BCNC/CuO/Graphene, adding Graphene did not result in new peaks. This situation makes it challenging to detect Graphene diffraction peaks using the intensity of the BCNC/CuO/Graphene composite [26,29–31].

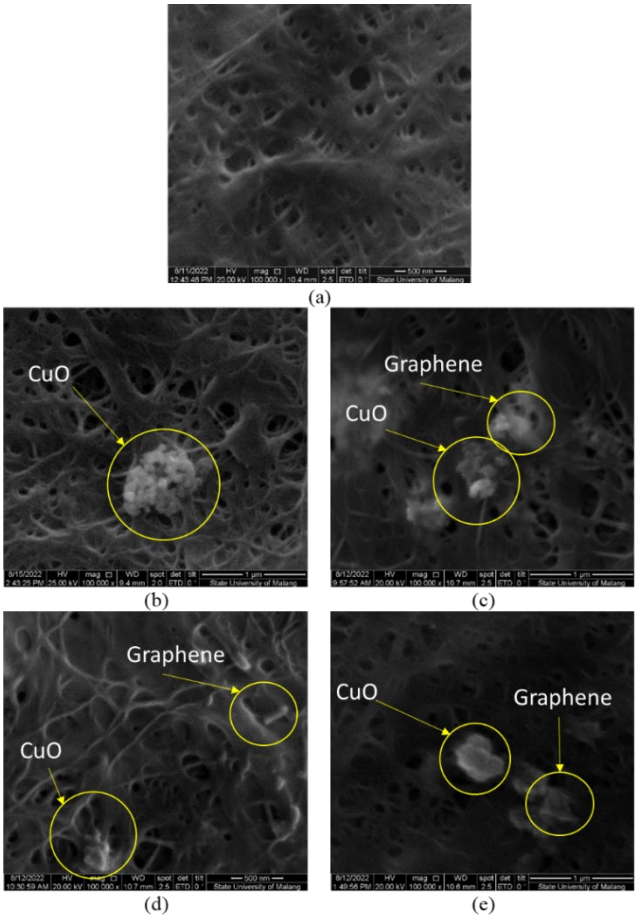

Fig 1: Morphology Bacterial Cellulose without addition (a), BCNC/CuO (b), BCNC/CuO/Graphene 0.1% (c), BCNC/CuO/Graphene 0.2% (d), BCNC/CuO/Graphene 0.3% (e)

The optimal amount of CuO and Graphene will be able to bind to cellulose, possibly breaking part of the bacterial cellulose crystal chain, whereas, in the BCNC/CuO/Graphene nanocomposite, the amount of Graphene that binds to cellulose decreases due to the addition of CuO composition so that Graphene will bind to CuO and not interfere bonding between cellulose. As a result, the crystallinity of cellulose increased. This increase in the crystallinity of cellulose indicated an improvement in cellulose structure, contributing to the enhancement of the mechanical strength of the BCNC [32].

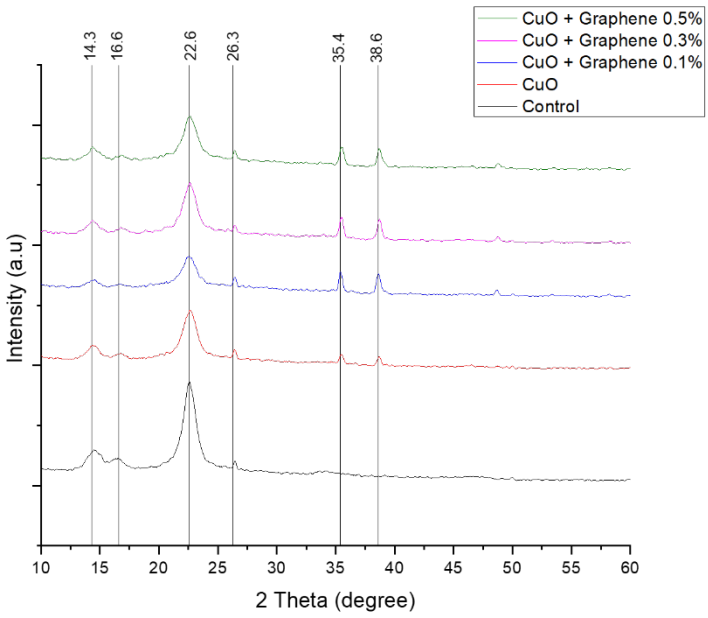

Fig 2: Crystallinity of BCNC/CuO/Graphene

Table 1 Intensity of BCNC/CuO/Graphene

Sample	Intensity in degree (a.u)					Crystallinity (%)	
	14.5º	**16.6º**	**22.6º**	**35.5º**	**38.7º**	**Cr**	**CI**
Control	187	125	470	-	-	88.84	87.44
BCNC + CuO-NPs	126	93	245	127	117	83.33	80
BCNC + CuO + Graphene 0.1%	103	86	214	124	112	80.45	75.70
BCNC + CuO + Graphene 0.3%	124	107	288	128	119	82.37	78.59
BCNC + CuO + Graphene 0.5%	130	95	266	130	125	84.79	82.06

Fourier Transform Infrared Analysis of BCNC/CuO/Graphene

Figure 3 shows troughs representing hydrogen bonding in the 3400-3500 cm^{-1} range (O-H stretching)[33]. The FTIR spectra at 3200 and 3500 cm^{-1} wavelengths indicate intramolecular hydrogen bonding of 3O-H-O5 bonds and the presence of hydroxyl groups[22,34]. Changes in the Carbonyl bonds in BCNC can also reveal the influence of Graphene addition [35]. The value of the C-H bond will be affected by Graphene of the alkyl type at wavelengths of 2902.86 cm^{-1}, 2981.29 cm^{-1}, 2899.01 cm^{-1}, 2908.65 cm^{-1}, and 2910.58 cm^{-1} [36].

Carbon triple bond (C≡C) The addition of Graphene causes modifications at wavelengths of 2133.27 cm^{-1}, 2131.34 cm^{-1}, 2135.19 cm^{-1}, and 2131.34 cm^{-1}. At wavelengths of 1597.05 cm^{-1}, 1598.98 cm^{-1}, 1595.20 cm^{-1}, 1595.13 cm^{-1}, and 1591.27 cm^{-1}, the presence of double bonds in aromatic carbon (C=O) is confirmed [31]. This decreased transmittance value indicates an increase in carbon and oxygen bonding, which are fundamental constituents of Graphene. There is a decrease in the peak in the wavelength range of 1600 cm^{-1}, 1475 cm^{-1}, 1087 cm^{-1} which is the value of the C = C bond[37]. Carbon elements in the C = C bond are released and cause the carbon

element to become open. This open carbon element will bind the oxygen element of CuO which ultimately causes an increase in the bond in the value range of 748 cm^{-1}. This bond is close to the transmittance value of the C(6)-O-Cu bond found in the value range of 748 cm^{-1} [38].

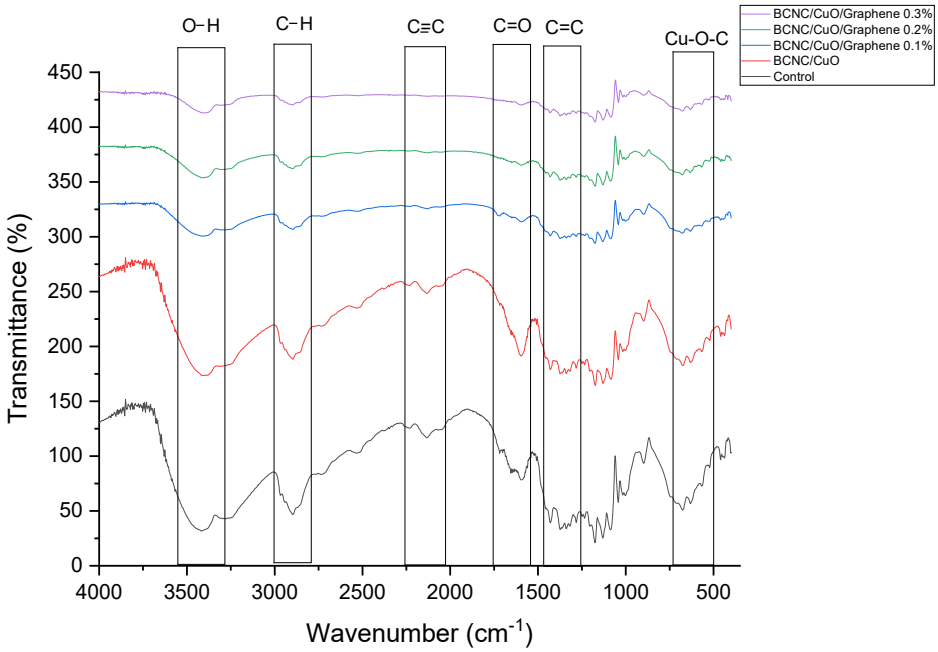

Fig 3: Transmittance of BCNC/CuO/Graphene

Mechanical Testing Analysis of BCNC/CuO/ Graphene

The addition of CuO to bacterial cellulose networks causes a decrease in the tensile strength value. It can be seen in the control sample that the tensile strength value produced is 40.652 MPa. After adding CuO, the mechanical strength becomes 26.707 MPa, then after adding Graphene 0.1% to 25.661 MPa, it rises to 40.436 MPa at 0.3% Graphene, and 42.479 at 0.5% Graphene. Based on the results of the stress value, it can be concluded that adding Graphene can increase the tensile strength of the nanocomposite membrane.

This result is also from previous research, which showed that the stress value increases with increasing Graphene concentration. Molecular interactions in the BCNC/CuO/Graphene nanocomposite network have an important role in changing the tensile strength value[39]. In BCNC/CuO, the effect of CuO addition can affect the C-H bond and the O-H molecular bond of bacterial cellulose, which is the main cellulose bond and becomes the foundation of the strength of the bacterial cellulose network [40].

Surface Roughness of BCNC/CuO/Graphene

Figure 5 and Tabel 2 presents the outcomes of a surface analysis conducted on BCNC membranes using a surface tester. A random sampling approach was employed to measure the roughness across the entire membrane during testing. Introducing CuO into the bacterial cellulose nanocomposite led to an increase in surface roughness. Specifically, the inclusion of CuO resulted in a 79% enhancement in roughness, yielding a roughness value of 4.81 micrometers. It's worth noting that the uneven distribution of CuO within the bacterial cellulose network contributed to the observed increase in surface roughness [41].

Table 2. Roughness of BCNC/CuO/Graphene

No	Sample	Roughness (Ra)
1	Control	2.68µm
2	BCNC + CuO-NPs	4.81 µm
3	BCNC + CuO + Graphene 0.1%	4.39 µm
4	BCNC + CuO + Graphene 0.3%	3.51 µm
5	BCNC + CuO + Graphene 0.5%	3.29 µm

Based on the results obtained from the morphological analysis using SEM, it was observed that the CuO and Graphene nanoparticles added to the bacterial cellulose network did not penetrate the pores within the network. This was primarily due to their tendency to agglomerate, causing them to gather and accumulate on the surface of the nanocomposite material instead [34]. The addition of Graphene decreases the roughness value compared to BC/CuO without Graphene. This is because the addition of Graphene to the CTAB and CuO network is able to reduce the ability of agglomeration between CuO materials. The presence of a Graphene layer around CuO causes a repulsive force between CuO so that the possibility for CuO to agglomerate is reduced. There is a indirect correlation between the surface roughness and membrane tensile strength. By reducing agglomeration, help the force distribution on BCNC to be better and able to accommodate forces from outside better so as to produce a stronger tensile strength[42,43].

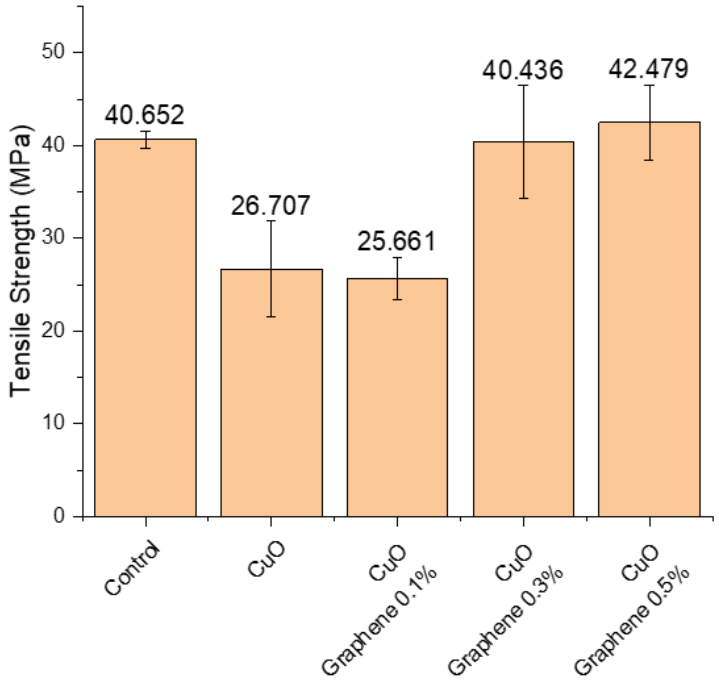

Fig 4: Tensile strength of BCNC/CuO/Graphene

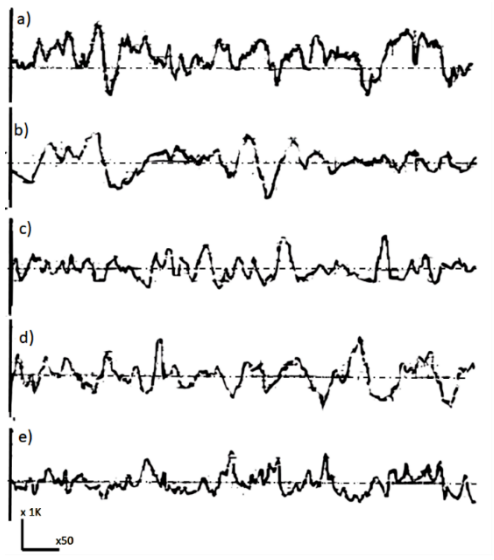

Fig 5: Surface roughness BCNC/CuO/Graphene

4. Conclusion

Agglomeration was observed at various locations when CuO and Graphene were attached to the Bacterial Cellulose Nanocomposite (BCNC). The amount of CuO added to the bacterial cellulose nanocomposite changed the resultant graph by adding additional peaks at 35.4° and 38.6° diffraction angles. The presence of Graphene reduces the crystallinity of bacterial cellulose. Changes in transmittance values at wavelengths 424, 499, 601, and 673 cm^{-1} can detect the BCNC/CuO functional groups. In contrast, the BCNC/CuO/Graphene molecular bonds can be detected by changes in the formation of valleys that are increasingly blunt at the 400-700 range, which represents the Cu-O-H bonds. Increasing the percentage of CuO in the BCNC/CuO causes agglomeration, which increases the roughness value of the BCNC/CuO. In the BCNC/CuO/Graphene, adding Graphene tends to decrease the roughness value compared to the BCNC/CuO. Based on the characterization performed,

BCNC/CuO/Graphene can be used as one of the filter candidates in future air circulation.

Acknowledgments

We want to express our gratitude to PNBP Universitas Negeri Malang, in particular, for providing funding for Penelitian Hibah Publikasi Tesis, whose contract number for a research project is 5.4.813/UN32.20.1/LT/2023.

References

1) Jenneke. Seddiqi, Hadi. Oliaei, Erfan. Honarkar, Hengameh. Jin, Jianfeng. Geonzon, Lester C. Bacabac, Rommel G. Klein-Nulend, "Cellulose and its derivatives: towards biomedical applications," *Cellulose*, 28 (*4*) 1893–1931 (2021). doi:10.1007/s10570-020-03674-w.
2) K. Pulidindi, and A. Prakash, "Cellulose market size and share | industry analysis - 2026," *Global Market Insight*, (2019).
3) D.F. Smaradhana, D. Ariawan, and R. Alnursyah, "A progress on nanocellulose as binders for loose natural fibres," *Evergreen*, 7 (*3*) 436–443 (2020). doi:10.5109/4068624.
4) C.W.Isidoro. Fernandes, Isabela de Andrade Arruda. Pedro, Alessandra Cristina. Ribeiro, Valéria Rampazzo. Bortolini, Débora Gonçalves. Ozaki, Mellany Sarah Cabral. Maciel, Giselle Maria. Haminiuk, "Bacterial cellulose: from production optimization to new applications," *Int J Biol Macromol*, 164 2598–2611 (2020). doi:10.1016/j.ijbiomac.2020.07.255.
5) H. Suryanto, T.A. Sutrisno, U. Yanuhar, and R. Wulandari, "Morphology and structure of bacterial cellulose film after ionic liquid treatment," *J Phys Conf Ser*, 1595 (*1*) (2020). doi:10.1088/1742-6596/1595/1/012028.
6) J. Gutierrez, A. Tercjak, I. Algar, A. Retegi, and I. Mondragon, "Conductive properties of tio 2/bacterial cellulose hybrid fibres," *J Colloid Interface Sci*, 377 (*1*) 88–93 (2012). doi:10.1016/j.jcis.2012.03.075.
7) M.P. Illa, C.S. Sharma, and M. Khandelwal, "Catalytic graphitization of bacterial cellulose–derived carbon nanofibers for stable and enhanced anodic performance of lithium-ion batteries," *Mater Today Chem*, 20 100439 (2021). doi:10.1016/j.mtchem.2021.100439.
8) S.A. Sardjono, H. Suryanto, Aminnudin, and M. Muhajir, "Crystallinity and morphology of the bacterial nanocellulose membrane extracted from pineapple peel waste using high-pressure homogenizer," in: AIP Conf Proc, 2019: pp. 1–5. doi:10.1063/1.5115753.
9) B.S. Rana, G. Bhushan, and P. Chandna, "The impact of nano fly ash particulates on tribological performance of jute /cotton fiber reinforced hybrid bio-composite," *Evergreen*, 10 (*3*) 1349–1356 (2023). doi:10.5109/7151682.
10) S.P. Dwivedi, A. Saxena, and S. Sharma, "Influence of nano-cuo on synthesis and mechanical behavior of spent alumina catalyst and grinding sludge reinforced aluminum based composite," *International Journal of Metalcasting*, 16 (*1*) 292–303 (2022). doi:10.1007/s40962-021-00597-5.
11) J. Maulana, H. Suryanto, and Suryanto, "Influence of copper oxide nanoparticles on properties of bacterial nanocellulose membrane made of pineapple peel waste," *Journal of Engineering Science and Technology Review*, 15 (*5*) 109–113 (2022). doi:10.25103/jestr.155.14.
12) G. Ren, D. Hu, E.W.C. Cheng, M.A. Vargas-Reus, P. Reip, and R.P. Allaker, "Characterisation of copper oxide nanoparticles for antimicrobial applications," *Int J Antimicrob Agents*, 33 (*6*) 587–590 (2009). doi:10.1016/j.ijantimicag.2008.12.004.
13) A.A. Iqbal, N. Sakib, A.K.M.P. Iqbal, and D.M. Nuruzzaman, "Graphene-based nanocomposites and their fabrication, mechanical properties and applications," *Materialia (Oxf)*, 12 (2020). doi:10.1016/j.mtla.2020.100815.
14) E. Rashidian, V. Babaeipour, A. Chegeni, N. Khodamoradi, and M. Omidi, "Synthesis and characterization of bacterial cellulose/graphene oxide nano-biocomposites," *Polym Compos*, 42 (*9*) 4698–4706 (2021). doi:10.1002/pc.26179.
15) M. Oprea, and D. Mihaela Panaitescu, "Nanocellulose hybrids with metal oxides nanoparticles for biomedical applications," *Molecules*, 25 (*18*) 4–6 (2020). doi:10.3390/molecules25184045.
16) M. Rashad, F. Pan, A. Tang, M. Asif, J. She, J. Gou, J. Mao, and H. Hu, "Development of magnesium-graphene nanoplatelets composite," *J Compos Mater*, 49 (*3*) 285–293 (2015). doi:10.1177/0021998313518360.
17) V. Ordonez, H. Baykara, A. Riofrio, M. Cornejo, and R. Rodríguez, "Preparation and characterization of ecuadorian bamboo fiber-low-density polyethylene (ldpe) biocomposites," *Evergreen*, 10 (*1*) 43–54 (2023). doi:10.5109/6781037.
18) M. Muhajir, H. Suryanto, Y.R.A. Pradana, and U. Yanuhar, "Effect of homogenization pressure on bacterial cellulose membrane characteristic made from pineapple peel waste," *Journal of Mechanical Engineering Science and Technology (JMEST)*, 6 (*1*) 34 (2022). doi:10.17977/um016v6i12022p034.
19) Brahmananda Reddy Sathi, Swami Naidu Gurugubelli, and Hari Babu N, "The effect of ecap on structural morphology and wear behaviour of 5083 al composite reinforced with red mud," *Evergreen*, 10 (*2*) 774–781 (2023). doi:10.5109/6792827.
20) L.D.S. Yadav, "Organic Spectroscopy," 2005th ed., Springer Science and Business Media B.V., allahabad, 2005. doi:10.1007/978-1-4020-2575-4.

21) D.S. Patil, and M.M. Bhoomkar, "Investigation on mechanical behaviour of fiber-reinforced advanced polymer composite materials," *Evergreen*, 10 (*1*) 55–62 (2023). doi:10.5109/6781040.
22) J. Maulana, H. Suryanto, and A. Aminnudin, "Effect of graphene addition on bacterial cellulose-based nanocomposite," *Journal of Mechanical Engineering Science and Technology (JMEST)*, 6 (*2*) 107 (2022). doi:10.17977/um016v6i22022p107.
23) H. Suryanto, U. Yanuhar, J. Maulana, and Y.R. Aji Pradana, "Effect of addition surfactant on properties of bacterial cellulose based composite foam reinforced by copper oxide nanoparticle," *Journal of Engineering Science and Technology Review*, 14 (*6*) 102–106 (2021). doi:10.25103/jestr.146.11.
24) Y. Li, D. Yang, and J. Cui, "Graphene oxide loaded with copper oxide nanoparticles as an antibacterial agent against: pseudomonas syringae pv. tomato," *RSC Adv*, 7 (*62*) 38853–38860 (2017). doi:10.1039/c7ra05520j.
25) P. Hidalgo-Manrique, X. Lei, R. Xu, M. Zhou, I.A. Kinloch, and R.J. Young, "Copper/graphene composites: a review," *J Mater Sci*, 54 (*19*) 12236–12289 (2019). doi:10.1007/s10853-019-03703-5.
26) H. Luo, G. Xiong, Z. Yang, S.R. Raman, H. Si, and Y. Wan, "A novel three-dimensional graphene/bacterial cellulose nanocomposite prepared by in situ biosynthesis," *RSC Adv*, 4 (*28*) 14369–14372 (2014). doi:10.1039/c4ra00318g.
27) H. Luo, J. Dong, X. Xu, J. Wang, Z. Yang, and Y. Wan, "Exploring excellent dispersion of graphene nanosheets in three-dimensional bacterial cellulose for ultra-strong nanocomposite hydrogels," *Compos Part A Appl Sci Manuf*, 109 290–297 (2018). doi:10.1016/j.compositesa.2018.03.007.
28) W. Shao, S. Wang, H. Liu, J. Wu, R. Zhang, H. Min, and M. Huang, "Preparation of bacterial cellulose/graphene nanosheets composite films with enhanced mechanical performances," *Carbohydr Polym*, 138 166–171 (2016). doi:10.1016/j.carbpol.2015.11.033.
29) H. Luo, H. Ao, G. Li, W. Li, G. Xiong, Y. Zhu, and Y. Wan, "Bacterial cellulose/graphene oxide nanocomposite as a novel drug delivery system," *Current Applied Physics*, 17 (*2*) 249–254 (2017). doi:10.1016/j.cap.2016.12.001.
30) R. Ikram, B.M. Jan, and W. Ahmad, "An overview of industrial scalable production of graphene oxide and analytical approaches for synthesis and characterization," *Journal of Materials Research and Technology*, 9 (*5*) 11587–11610 (2020). doi:10.1016/j.jmrt.2020.08.050.
31) E. Rashidian, V. Babaeipour, A. Chegeni, N. Khodamoradi, and M. Omidi, "Synthesis and characterization of bacterial cellulose/graphene oxide nano-biocomposites," *Polym Compos*, 42 (*9*) 4698–4706 (2021). doi:10.1002/pc.26179.
32) D. Ariawan, W.P. Raharjo, K. Diharjo, W.W. Raharjo, and B. Kusharjanta, "Influence of tropical climate exposure on the mechanical properties of rhdpe composites reinforced by zalacca midrib fibers," *Evergreen*, 9 (*3*) 662–672 (2022). doi:10.5109/4842526.
33) V.A. Gandhari, M.S. Perdani, and H. Hermansyah, "Improvement on reusability, storage stability and thermal stability of magnetic graphene oxide-immobilized cholesterol oxidase," *Evergreen*, 9 (*2*) 500–505 (2022). doi:10.5109/4794178.
34) H. Suryanto, B.D. Susilo, J. Maulana, and U. Yanuhar, "Characterization of nanocomposite membrane based bacterial cellulose made of pineapple waste reinforced by graphite nanoplatelets," 1–11 (2022). doi:10.32604/jrm.2022.020478.
35) A.H. Wibowo, H. Al Arraf, A. Masykur, F. Rahmawati, M. Firdaus, F. Pasila, U. Farahdina, and N. Nasori, "Composite of polyaniline / reduced graphene oxide with the single- , bi- and tri- metal oxides modification and the effect on the capacitance properties," 10 (*01*) 85–93 (2023).
36) A. Mensah, P. Lv, C. Narh, J. Huang, D. Wang, and Q. Wei, "Sequestration of pb(ii) ions from aqueous systems with novel green bacterial cellulose graphene oxide composite," *Materials*, 12 (*2*) (2019). doi:10.3390/ma12020218.
37) A.H. Wibowo, H. Al Arraf, A. Masykur, F. Rahmawati, M. Firdaus, F. Pasila, U. Farahdina, and N. Nasori, "Composite of polyaniline/reduced graphene oxide with the single-, bi- and tri- metal oxides modification and the effect on the capacitance properties," *Evergreen*, 10 (*1*) 85–93 (2023). doi:10.5109/6781053.
38) Ž. Mitić, G.S. Nikolić, M. Cakić, P. Premović, and L. Ilić, "FTIR spectroscopic characterization of cu(ii) coordination compounds with exopolysaccharide pullulan and its derivatives," *J Mol Struct*, 924–926 (*C*) 264–273 (2009). doi:10.1016/j.molstruc.2009.01.019.
39) H. Sosiati, N.D.M. Yuniar, D. Saputra, and S. Hamdan, "The influence of carbon fiber content on the tensile, flexural, and thermal properties of the sisal/pmma composites," *Evergreen*, 9 (*1*) 32–40 (2022). doi:10.5109/4774214.
40) D. Fengel, "Characterization of cellulose by deconvoluting the oh valency range in ftir spectra," *Holzforschung*, 46 (*4*) 283–288 (1992). doi:10.1515/hfsg.1992.46.4.283.
41) W. He, Z. Zhang, Y. Zheng, S. Qiao, Y. Xie, Y. Sun, K. Qiao, Z. Feng, X. Wang, and J. Wang, "Preparation of aminoalkyl-grafted bacterial cellulose membranes with improved antimicrobial properties for biomedical applications," *J Biomed Mater Res A*, 108 (*5*) 1086–1098 (2020). doi:10.1002/jbm.a.36884.
42) P.P. Selakjani, M. Peyravi, M. Jahanshahi, H. Hoseinpour, A.S. Rad, and S. Khalili, "Strengthening

of polysulfone membranes using hybrid mixtures of micro- and nano-scale modifiers," *Front Chem Sci Eng*, 12 (*1*) 174–183 (2018). doi:10.1007/s11705-017-1670-y.

43) M. Agtaş, T. Ormancı-Acar, B. Keskin, T. Türken, and I. Koyuncu, "Nanofiltration membranes for salt and dye filtration: effect of membrane properties on performances," *Water Science and Technology*, 83 (*9*) 2146–2159 (2021). doi:10.2166/wst.2021.125.